Persistent spectral hole burning in semiconductor nanocrystals

Kazuhiko Naoe,* Lev G. Zimin,† and Yasuaki Masumoto‡
Institute of Physics, University of Tsukuba, Tsukuba, Ibaraki 305, Japan
(Received 14 April 1994; revised manuscript received 13 July 1994)

A persistent spectral hole-burning phenomenon in nanometer-size semiconductor microcrystals (nanocrystals), namely, CdSe, $CdS_{0.59}Se_{0.41}$, and CuCl, embedded in a crystal or glass was observed. When the spectrally narrow laser excites the inhomogeneously broadened absorption band of CdSe and CuCl nanocrystals, a narrow bleaching hole and induced absorption arise in the absorption spectra at 2 K and are present for more than a few hours after the laser irradiation. Long-lived bleaching was observed also in $CdS_{0.59}Se_{0.41}$ nanocrystals together with photodarkening. A photophysical model explains the long-lived bleaching ascribed to the spectral antihole fairly well, but some part of the persistent spectral hole burning comes from the photochemical mechanism. Nanocrystals consisting of 10^3–10^4 atoms behave like molecules or ions in a matrix to give the persistent spectral hole-burning phenomenon. This means that the total system consisting of even one semiconductor nanocrystal and the matrix has more than one ground-state configuration. Not only the size distribution but also these ground-state configurations give inhomogeneous broadening to semiconductor nanocrystals.

I. INTRODUCTION

Nanometer-size semiconductor crystals are known as zero-dimensional quantum dots. The nanocrystals have been prepared by several kinds of growth methods: ion aggregation growth in glass and crystals, interrupted growth of colloidal particles in solvents, electron-beam lithography, and so on. When photoexcited electrons and holes or excitons are confined to semiconductor nanocrystals, their electronic and optical properties are strongly changed. Their optical properties have been explained by the quantum confinement effect.[1–3] In recent years, the nonlinear optical properties of zero-dimensional systems have been extensively studied by means of both experimental and theoretical approaches, because they have unique properties and a potential for device applications.[4–6]

In semiconductor nanocrystal samples, the absorption band is inhomogeneously broadened. The origin of the inhomogeneous broadening has been explained by the size distribution of semiconductor nanocrystals, while we may consider the other origins of the inhomogeneous broadening for semiconductor nanocrystals, because they are made of as small as $10^3 \sim 10^6$ atoms like macromolecules. In fact, in transparent glass, crystals, and polymers containing absorbing molecular or ionic guests, the origins of the inhomogeneous broadening are the distribution of local environments due to structural randomness, crystal field, and strains.[7]

When the spectrally narrow light excites materials having the inhomogeneously broadened absorption band, a spectral hole in the absorption band is formed at the position of the excitation photon energy. This phenomenon is called spectral hole burning. Spectral hole burning is often used to study the homogeneous line broadening, because the homogeneous linewidth can be estimated from the spectral hole.[8] The spectral hole-burning spectroscopy reveals the electron and exciton dynamics, carrier-surface interactions, carrier-phonon interactions, etc. in nanocrystals. Therefore, much work has been performed to study semiconductor nanocrystals by means of the hole-burning spectroscopy.[9–16]

For CdSe nanocrystals, the homogeneous linewidth in CdSe embedded into polymer is narrow compared with that in CdSe embedded in glass.[10–13,15] Therefore, this difference between glass and polymer samples originates from surrounding matrix materials.[10–13] Organometallic reactions at surface can be utilized to produce nanocrystals which are passivated or capped by organic groups simultaneously. Contrary to the organic matrix, the chemical understanding of the glass-nanocrystal interface is rather poor. There are several reports on CdSe nanocrystals embedded in glass concerning carrier dynamics,[12] surface effects,[13,15] and carrier-phonon interactions.[9,17] However, there is still no consensus of the origin of the homogeneous broadening of semiconductor nanocrystals. In CuCl nanocrystals embedded into NaCl crystals, the homogeneous linewidth is much narrower than that of CdSe nanocrystals and the size dependence of the homogeneous linewidth has been reported.[14,18] It has been shown that the size dependence of homogeneous linewidth is inversely proportional to the square of the radius of nanocrystals. The interaction of confined excitons with surfaces and phonons is important for the broadening. Moreover, the confined phonons in nanocrystals were recently observed by using pump-and-probe method.[19] However, it is strange that the hole-burning spectra consist of a narrow spectral hole and the broad bleaching band.[20,21] The phenomenon cannot be understood on the basis of the power broadening model.[8]

Therefore, we need study the homogeneous and inhomogeneous broadening of semiconductor nanocrystals embedded in matrices from a different standing point. So far, the spectral hole-burning phenomenon observed in semiconductor nanocrystals has been believed to be transient. However, we found the persistent spectral hole

0163-1829/94/50(24)/18200(11)/$06.00

burning (PSHB) phenomenon in semiconductor nanocrystals. In the preceding paper,[22] we briefly reported this finding. In this paper, we report the phenomenon much more extensively. The understanding of the phenomenon serves to solve the above-mentioned questions about the hole burning. The layout of this paper is as follows: In Sec. II, two underlying backgrounds concerning this work are described. In Sec. III, the experimental procedures for the measurements of spectral hole burning are explained. In Sec. IV, the experimental results are described and discussion is made. First, the excitation energy dependence of differential absorption spectra is shown in CdSe nanocrystals embedded in GeO_2 glass. Second, the observation of PSHB is presented for four types of semiconductor nanocrystal samples (CdSe nanocrystals in GeO_2 glass, $CdSe_{0.59}S_{0.41}$ nanocrystals in glass, and CuCl nanocrystals in glass and in NaCl). Third, the PSHB mechanism in semiconductor nanocrystals is discussed. Finally, the demonstration experiment of the optical data storage in CuCl nanocrystals embedded in glass is shown. In Sec. V, the results, conclusions, and impacts of this work are summarized.

II. UNDERLYING BACKGROUNDS

A. Quantum-size effects of semiconductor nanocrystals

The finite size of nanocrystals leads to an increase in the kinetic energy of confined electrons, holes, and excitons.[1-3] Depending on the relative size of the radius of a nanocrystal R compared with the exciton Bohr radius a_B, there are two limiting cases. One of them is the so-called "weak confinement" regime, where $R \gg a_B$ holds. This is typically observed in CuCl nanocrystals where the bulk exciton Bohr radius a_B is 0.68 nm. The lowest-energy state of this system can be expressed as a function of R as follows:

$$E = E_g + \frac{\hbar^2}{2M}\frac{\pi^2}{(R-\eta a_B)^2} - E_R, \quad M = m_e^* + m_h^* , \tag{1}$$

where E_g is the bulk energy gap, M is the translational mass of exciton, E_R is the Rydberg energy, and m_e^* (m_h^*) is an effective mass of the electron (hole). The a_B multiplied by η corresponds to the dead layer for excitons. For CuCl nanocrystals, $E_g - E_R = 3.2025$ eV (2 K), $E_R = 213$ meV, $M = 2.3m_0$, and $\eta = 0.5$ are used, where m_0 is the electron mass.

The other case is known as the "strong confinement" regime, where $R \ll a_B$ holds. Both electrons and holes are quantized separately and, for example, CdSe nanocrystals are treated on this model. The lowest energy of this system as a function of R can be expressed by

$$E = E_g + \frac{\hbar^2\pi^2}{2\mu R^2} - \frac{1.786e^2}{\varepsilon R} - 0.248E_R , \qquad \frac{1}{\mu} = \frac{1}{m_e^*} + \frac{1}{m_h^*} , \tag{2}$$

where ε is a dielectric constant of the semiconductor. The second term of the right-hand side is due to quantum confinement of electron and hole, the third term means the Coulomb energy, and the last term means the correlation energy. For CdSe nanocrystals, $E_g = 1.841$ eV (A band), $E_R = 15.7$ meV, $\mu = 0.12m_0$, and $\varepsilon = 9.3$ are used. Both Eqs. (1) and (2) show that the lowest energy increases with the decrease in the radius R of nanocrystals. Nanocrystals in samples have the size distribution. Therefore, the size distribution leads to the inhomogeneous broadening of the absorption spectra. So far, the size distribution is considered to be the unique origin of the inhomogeneous broadening of nanocrystals.[3]

B. Persistent spectral hole burning

Spectrally narrow excitation of the inhomogeneously broadened absorption band in materials permits us to observe the spectral hole. In some kinds of solids, the spectral hole is preserved for time periods longer than the lifetime of any excited state. This phenomenon is called "persistent spectral hole burning (PSHB)."[7] The PSHB is observed in a number of transparent hosts, glass, crystals, and polymers, containing absorbing ionic or molecular guests. Basic requirements for the PSHB are as follows: (1) The optical absorption of a guest embedded in a host must be broadened inhomogeneously. (2) There must exist more than one ground-state configuration of the total system consisting of a guest and a host. (3) The relaxation among the ground states must be slower than the decay rate of any excited state.

Microscopic mechanism leading to the PSHB phenomenon can be roughly classified into two categories: photochemical[23-28] and nonphotochemical (photophysical) mechanisms.[29-32] Photochemical mechanisms usually involve some internal changes in the guest center itself, such as bond breaking, ionization, isomerization, tautomerization, and so forth. Nonphotochemical (photophysical) mechanisms arise from a change in environment around the guest. Especially, it is known that amorphous hosts, glass and polymers, play an important role for photophysical hole burning. They are simplified into the so-called two-level system defined by double-well potential[29,30,32] for understanding of the phenomena. There has been much work to clarify the mechanisms of the PSHB. Nevertheless, there are many unknown parts concerning the PSHB mechanisms up to now.

III. EXPERIMENTAL PROCEDURES

A. Samples

In this paper, four kinds of semiconductor nanocrystals were studied by means of hole-burning spectroscopy. They are CdSe in GeO_2 glass ($R = 2.4$ nm), $CdS_{0.59}Se_{0.41}$ in SiO_2-rich glass ($R = 4.0$ nm), CuCl in a NaCl crystal ($R = 2.7$ nm), and CuCl in SiO_2-rich glass ($R = 2.5$ nm). The mean size of nanocrystals in four samples was determined by small-angle x-ray-scattering measurements.

The preparation method of the sample, CdSe in GeO_2 glass, was described in Ref. 33. In order to check the difference in the hole-burning behavior depending on the host glass, CdS_xSe_{1-x} nanocrystals in silica-rich glass

were also prepared.[34] The composition of $CdS_{0.59}Se_{0.41}$ was determined by the Raman shift of the LO phonon.[35]

Samples, CuCl nanocrystals in NaCl, were made from the melt mixture of NaCl powder and CuCl powder and grown by the transverse Bridgman method. After this process, the sample was annealed to control the size of CuCl nanocrystals. Many researches on optical properties of confined excitons, phonons, and biexcitons have been performed in the same type of CuCl nanocrystals.[14,18,19,36–38] The other nanocrystals were CuCl nanocrystals in aluminoborosilicate of glass. The size of CuCl nanocrystals was also controlled by means of heat treatment.[39]

B. Nanosecond pump-and-probe measurements

In pump-and-probe experiments, the change in absorption can be measured and expressed as the form of different absorption spectrum (DAS). The differential absorption spectrum, $-\Delta\alpha d$, is defined as

$$-\Delta\alpha d=(\alpha d)_0-(\alpha d)_{\text{pump}}$$
$$=-\ln\frac{I_{\text{probe}}}{I_{\text{ref}}}-\left[-\ln\frac{I_{\text{p·p}}-I_{\text{pump}}}{I_{\text{ref}}}\right],$$

where $(\alpha d)_0$ and $(\alpha d)_{\text{pump}}$ are absorbance of the sample without and with a pump beam, respectively. I_{ref} represents the intensity of the probe beam. I_{probe} and $I_{\text{p·p}}$ represent the measured transmitted intensity of the probe beam through the sample without and with a pump beam, respectively. I_{pump} represents the intensity of pump-beam scattering and photoluminescence. Because the pump intensity is much larger than the probe intensity, $I_{\text{p·p}}$ involves the effects of pump-beam scattering and photoluminescence. Therefore, we omit them by subtracting I_{pump} from $I_{\text{p·p}}$ as shown in the second term in the above expression. We neglect the intensity profile of the pump laser in the samples.

A dye laser pumped by the second or the third harmonics of the output of a Q-switched Nd^{3+}:YAG (yttrium aluminum garnet) laser was used as a pump source. The spectral linewidth of the dye laser was 0.001 nm (0.006 meV) around 3.2 eV and 0.002 nm (0.007 meV) around 2.2 eV and the pulse duration was approximately 5 ns. As for laser dyes, we used Coumarin 153 and Rhodamine 6G for CdSe and $CdS_{0.59}Se_{0.41}$ nanocrystals and Exalite 384 for CuCl nanocrystals. As the probe source, amplified spontaneous emission (ASE) from dye solution was used. The ASE was excited by a portion of the output of the Q-switched Nd^{3+}:YAG laser. A few kinds of dyes were mixed in order to broaden the spectral range of the probe beam. The optical delay was adjusted to reduce the time delay between pump and probe pulses to less than 1 ns. Nanosecond pump-and-probe experiments at zero time-delay were done without a chopper. For time-resolved measurements, a special chopper which was constituted by a chopper blade having three series of holes was used. This chopper was synchronized with the Q-switched Nd^{3+}:YAG laser. Both pump-and-probe pulses alternately passed through the chopper. The chopper providing the trigger pulses to the laser could give the time delay between pump-and-probe pulses in the millisecond regime. To increase the time delay, the chopper blade was changed. In this way, the delay was varied from 0 to 1.4 s. Polarizers and spatial apertures were employed to reduce the pump-beam scattering in all experiments. The spot of the probe beam on the sample was approximately 300 μm in diameter and was spatially overlapped with the pump beam which was about 500 μm in diameter.

The samples were directly immersed in superfluid helium at 2 K or in liquid nitrogen at 77 K. The transmittance of the probe beam was detected by using an optical multichannel analyzer (OMA) in conjunction with a 25-cm monochromator or a 93-cm monochromator. The spectral resolution of the experiment was approximately 3 nm (11 meV) for CdSe and $CdS_{0.59}Se_{0.41}$ samples and 0.2 nm (1.6 meV) for CuCl samples.

IV. EXPERIMENTAL RESULTS AND DISCUSSIONS

A. Excitation energy dependence

Excitation energy dependence of the differential absorption spectrum (DAS) in CdSe nanocrystals embedded in GeO_2 glass was measured without the chopper. The pump-and-probe pulses were adjusted to reach the sample simultaneously. The upper part and the lower part of Fig. 1 show a linear absorption spectrum and the DAS at 2 K, respectively. In the linear absorption spectrum, two

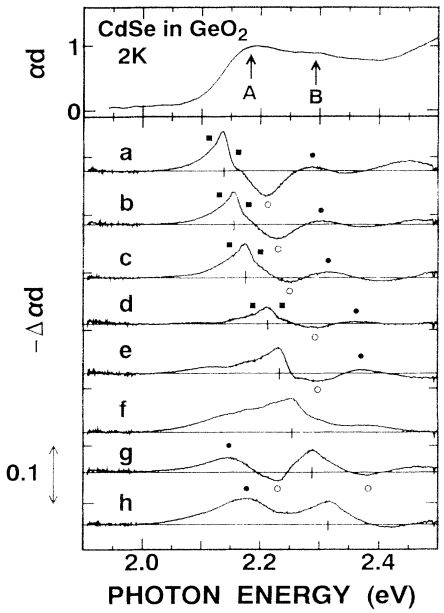

FIG. 1. The upper part is the linear absorption spectrum of CdSe nanocrystals embedded in GeO_2 glass at 2 K. *A* band and *B* band are indicated by arrows. The lower part shows differential absorption spectra in the same sample at 2 K. The energy positions of the excitation are indicated by vertical bars [(a) 2.138 eV, (b) 2.156 eV, (c) 2.175 eV, (d) 2.214 eV, (e) 2.234 eV, (f) 2.254 eV, (g) 2.288 eV, and (h) 2.317 eV]. The excitation energy density was approximately 0.15~0.25 mJ/cm^2. The open circles and the solid circles indicate antiholes and satellite holes, respectively. The solid squares show the phonon sideband holes.

bands indicated by the arrows correspond to the lowest-energy quantum states of the A band and B band, similarly to the identification by previous authors.[12,13] The A band peak located at 2.19 eV is shifted by 370 meV from the bulk value of 1.826 eV. The blueshift is explained by Eq. (2), assuming that the radius of nanocrystals is 2.7 nm. The value almost agrees with the mean radius of 2.4 nm measured by the small-angle x-ray scattering. A-band and B-band peaks in the linear absorption spectrum are broadened inhomogeneously.

The DAS was obtained by changing the energy of the narrow-band excitation. The excitation energy density was approximately 0.15–0.25 mJ/cm^2. The excitation energy positions are indicated by the vertical bars in Fig. 1. According to Eq. (2), the excitation means the excitation of a certain-size nanocrystal. The A band was excited in the spectra (a)–(e). On the other hand, the B band was excited in (g) and (h). In spectrum (f), the energy position between A band and B band was excited. In our case, the shape and the linewidth of the spectral hole in the DAS are similar to those reported in CdSe nanocrystals in glass.[15,16] The spectral hole is about twice as narrow as previous reports in CdSe nanocrystals in glass.[12,13] These facts imply that the hole structure is not determined by the CdSe nanocrystals alone but by both the CdSe nanocrystals and the surrounding materials. Moreover, these spectra have rich structures: satellite holes and antiholes. The satellite hole is the bleaching structure at the different energies from the excitation energy. The antihole is the dip structure, which means induced absorption.

In order to assign these structures, the energy positions of antiholes and satellite holes are plotted in Fig. 2. The open circles and solid circles indicate the energy position of antiholes and satellite holes, respectively. The solid line represents the excitation energy. The five data from the left-hand side are taken from the spectra (a)–(e) in Fig. 1 and the others are from (g) and (h). As shown in Fig. 2, the energy difference between the excitation and the satellite holes taken from the spectra (a)–(e) in Fig. 1 is approximately 140 meV. In the linear absorption spectrum, the energy difference between the A-band peak and the B-band peak is estimated to be between 110 and 150 meV. This value almost agrees with the previously reported value for similar-size CdSe nanocrystals.[12,13] Therefore, it is reasonable that the satellite holes are attributable to the B band. When the A band is bleached, the B band is also bleached, because both the A band and the B band are made of the same conduction-band electron. Similarly, spectra (g) and (h) in Fig. 1 are understood, because the energy difference between the excitation and the satellite holes is also approximately 140 meV. The satellite holes in the spectra (g) and (h) originate from the A band.

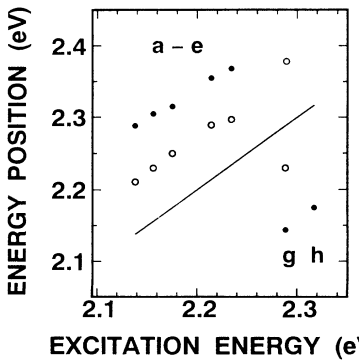

FIG. 2. Excitation energy dependence of the energy positions of antiholes (○) and satellite holes (●). The five data from the left-hand side are taken from spectra (a)–(e) and the others are from (g) and (h) in Fig. 1.

Figures 1 and 2 show that the high-energy-side antihole shifts in the similar manner to the main hole. Moreover, a new low-energy-side depth arises, when the main hole becomes rather far from the absorption edge. There is a model to explain the origin of antiholes.[12,13,40] On the basis of the model, the antihole is the induced absorption due to the generation of two-electron-hole-pair states.[12,13,15,16,40] Two-electron-hole-pair states may be generated by the absorption of both the pump photon and the probe photon. However, this model conflicts with the observed persistency of the antiholes which is presented in Sec. IV B.[41] In order to explain our results, another model is required. We discuss it in the next section.

The spectral holes in Fig. 1 are asymmetric, not Lorentzian, due to phonon sidebands. The LO- and TO-phonon energies in bulk CdSe are 26 meV and 21 meV, respectively.[42] It can be seen from the spectra (a)–(d) in Fig. 1 that there are shoulders marked by solid squares at the higher- and lower-energy sides of the spectral hole. The energy difference between the shoulders and the excitation energy is approximately 26 meV. Therefore, these shoulders of the spectral holes are considered to correspond to the structures due to optical phonons.

B. Observation of the persistent spectral hole-burning phenomena

In order to clarify the carrier dynamics in semiconductor nanocrystals, many studies have been done by means of the time-resolved spectroscopy. In CdSe nanocrystals, time-resolved luminescence has been investigated under picosecond excitation of the lowest excited state.[43] The emission showed two decay components with time constants of 110 ps and microsecond. The microsecond decay component was suggested to originate from the localization of excited carriers. Time-resolved pump-and-probe measurements were also done in CdSe nanocrystals.[11,12] Authors found that the bleaching structure lasts more than 500 ps (Ref. 12) or 40 ns.[11] The long decay was ascribed to the slow recombination of the trapped carriers.

1. Persistent spectral hole burning in CdSe nanocrystals

Figure 3 shows a linear absorption spectrum, (a), and DAS (differential absorption spectra), (b) and (c), in CdSe nanocrystals embedded in GeO_2 glass at 2 K. The time lag between pump and probe pulses in (b) was less than 1

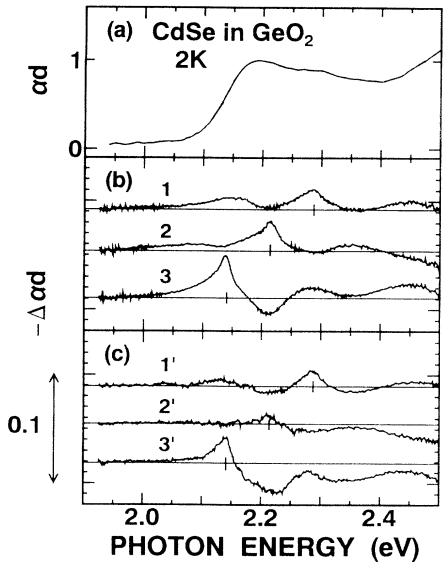

FIG. 3. Linear absorption spectrum (a) and the differential absorption spectra, (b) and (c), in CdSe nanocrystals embedded in GeO_2 glass at 2 K. The time delays in (b) and (c) were 0 and 33 ms, respectively. The excitation energy is indicated by vertical bars [1(1'):2.288 eV, 2(2'):2.214 eV, 3(3'):2.138 eV]. The excitation energy density was 25 $\mu J/cm^2$.

ns. The time delay in (c) was 33 ms. The repetition rates of both pump and probe pulses were 30 Hz for (b) and 15 Hz for (c). The relative timing between pump and probe pulses for (c) is illustrated in Fig. 4(a). The excitation energy of 1 (1'), 2 (2'), and 3 (3') was 2.288, 2.214, and 2.138 eV, respectively. The excitation energy density was 25 $\mu J/cm^2$ in all measurements. Figure 3 points out that the spectrum (c) and the spectrum (b) are alike in the structures of holes, satellite holes, and antiholes. It means that antiholes do not originate from the excited state of biexciton,[40] because the one-electron-hole pair state should completely disappear within much less than

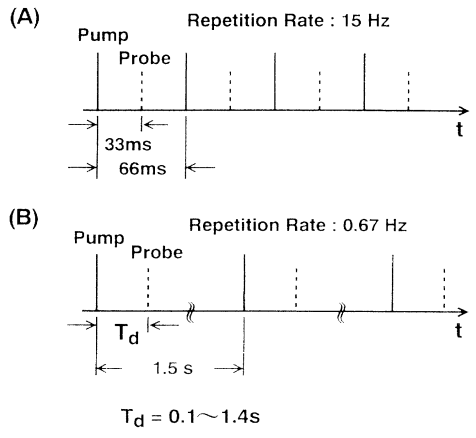

FIG. 4. The relative timing between pump-and-probe pulses for the time-resolved measurements. (a) The temporal sequence of pump-and-probe measurements in Fig. 3(c). (b) The temporal sequence of the pump-and-probe measurements in Figs. 5–12. The delay time is represented by T_d.

33 ms in direct-allowed semiconductor nanocrystals.[41]

Figure 5 shows the time dependence of DAS. The excitation photon energy and the excitation energy density were 2.175 eV and 1.0 mJ/cm^2, respectively. The repetition rates of both pump-and-probe pulses were reduced to 0.67 Hz. In this case, the relative timing between pump-and-probe pulses is illustrated in Fig. 4(b). The delay time of probe pulses for spectra (a), (b), and (c) in Fig. 5 were 0, 0.1, and 1.4 s, respectively. The dip structure in 0-s spectrum is swelled up compared with Fig. 1(c) as a result of the increase in the pump intensity. Spectral change takes place within 0.1 s and becomes small after 0.1 s. Figure 6 shows the temporal change in the intensity of the spectral hole for the same sample. This figure shows that the spectral hole was decreased quickly within 0.1 s and it becomes almost constant after 0.3 s. The most important point is that the spectral hole and the antihole are observed even at 1.4 s after the excitation. Moreover, it was found that the hole was still present after a few hours.

So far, the relaxation of the spectral hole (bleaching) in semiconductor nanocrystals has been explained by carrier relaxation processes from excited states.[9–16,20,21] The longest lifetime among the previous reports on CdSe nanocrystals is several microseconds which was explained by the localization of the excited carriers. However, in the present study, we observed that the spectral hole was held more than a few hours. This long-lived spectral hole cannot be explained by considering carrier relaxation processes from any excited states in CdSe nanocrystals. On the other hand, it is a well-known phenomenon that the spectral hole remains persistently in various kinds of materials.[7] This phenomenon is explained by PSHB. Therefore, it is reasonable to consider that the long-lived spectral holes in CdSe nanocrystals are explained by the PSHB process.

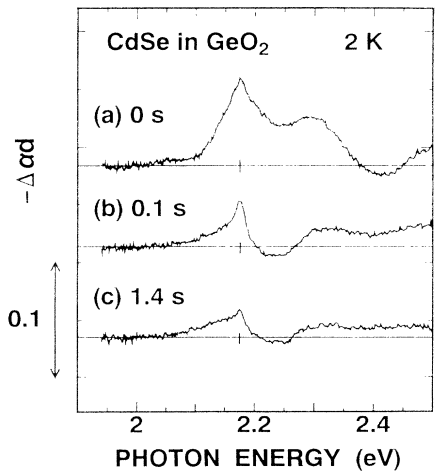

FIG. 5. The time dependence of the differential absorption spectra in CdSe nanocrystals embedded in GeO_2 glass at 2 K. The excitation photon energy shown by vertical bars and the excitation energy density were 2.175 eV and 1.0 mJ/cm^2, respectively. The repetition rate was 0.67 Hz. The delay time for spectra (a), (b), and (c) was 0, 0.1, and 1.4 s, respectively.

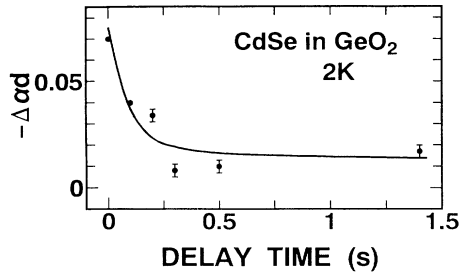

FIG. 6. The temporal change in the depth of spectral holes in CdSe nanocrystals embedded in GeO_2 glass at 2 K. The experimental conditions were the same as those of Fig. 5.

The phenomenon depends on the matrix. We examined another sample $CdS_{0.59}Se_{0.41}$ nanocrystals embedded into silica-rich glass. Figure 7 shows a linear absorption spectrum (a) and the time dependence of DAS (b) at 2 K in $CdS_{0.59}Se_{0.41}$ nanocrystals embedded in glass. The experimental condition was the same as that for CdSe in GeO_2 glass. The upper and the lower spectra in (b) were measured without and with 0.1-s time delay, respectively. The excitation energy and excitation energy density were 2.300 eV and 1.0 mJ/cm^2, respectively. At zero time delay, the distinct hole and the antihole are observed. On the contrary, the structure is weaker than the noise level at 0.1 s after the excitation. We were afraid that the probe pulses were erasing the spectral hole and, therefore, used the weak spectrally filtered output of the incandescent lamp which passed through a short-wavelength-cut filter (HOYA Y43) as the probe. The result is shown in (c). The excitation density of the pump pulses was 0.15 mJ/cm^2. After pump pulses hit the sample for 10 min, the pump was stopped. Then, the absorption spectrum was taken by accumulating the transmitted signal of the probe light for 20 min. The spectral hole was overlapped on the photodarkened spectrum and almost the same spectrum was also taken at 20 min after the laser excitation. This result is not enough to clarify the relationship between the PSHB and the photodarkening in this sample. However, it is obvious that the PSHB is a different phenomenon from the photodarkening and that the PSHB takes place in the $CdS_{0.59}Se_{0.41}$ in a glass sample, too.

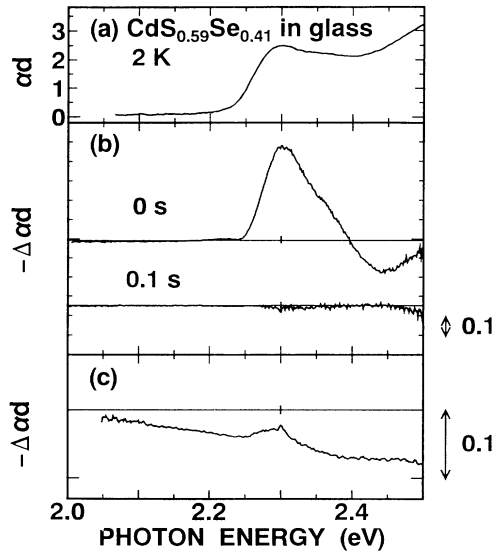

FIG. 7. (a) Linear absorption spectrum in $CdS_{0.59}Se_{0.41}$ nanocrystals embedded in silica-rich glass at 2 K. (b) The time dependence of the differential absorption spectra in the same sample at 2 K. The lower spectrum and the upper spectrum were measured with 0- and 0.1-s time delay, respectively. The excitation photon energy shown by vertical bars and the excitation energy density were 2.300 eV and 1.0 mJ/cm^2, respectively. The repetition rate was 0.67 Hz. (c) The absorbance change of the same sample at 2 K taken by using an incandescent lamp. The excitation photon energy and the excitation energy density were 2.300 eV and 0.15 mJ/cm^2, respectively. After pump pulses hit the sample for 10 min, the pump was stopped. Then, we started accumulating the transmitted spectrum in 1 min and the accumulation time was 20 min.

2. *Persistent spectral hole burning in CuCl nanocrystals*

Figures 8(a) and 9(a) show 2 K linear absorption spectra of CuCl nanocrystals embedded in glass and in NaCl, respectively. The broad structures indicated by arrows are due to the Z_3 exciton. These structures show blueshifts compared with the Z_3-exciton energy in bulk CuCl. The blueshift in Fig. 8(a) is 48 meV, which corresponds to the exciton quantum confinement energy in CuCl nanocrystals whose radius is 2.2 nm. This correspondence is obtained on the basis of Eq. (1) and the estimated value of 2.2 nm almost agrees with the value, 2.5 nm, obtained by the small-angle x-ray-scattering measurement. It is be-

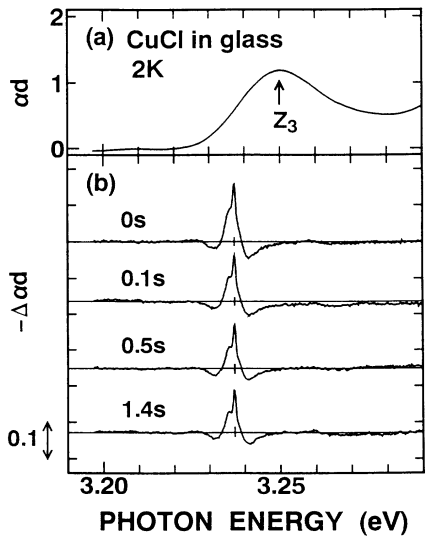

FIG. 8. (a) Linear absorption spectrum in CuCl nanocrystals embedded in glass at 2 K. The Z_3-exciton band is indicated by the arrow. (b) The time dependence of the differential absorption spectra in the same sample at 2 K. The excitation energy shown by vertical bars and the excitation energy density were 3.237 eV and 1.0 mJ/cm^2, respectively. The repetition rate was 0.67 Hz. The delay time was 0, 0.1, 0.5, and 1.4 s.

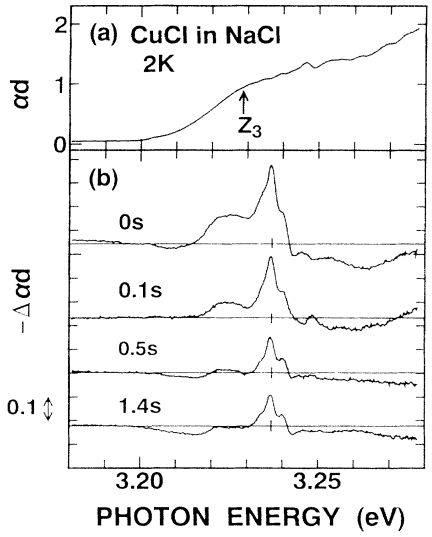

FIG. 9. (a) Linear absorption spectrum in CuCl nanocrystals embedded in NaCl at 2 K. The Z_3-exciton band is indicated by the arrow. (b) The time dependence of the differential absorption spectra in the same sample at 2 K. The excitation photon energy shown by vertical bars and the excitation energy density were 3.237 eV and 1.5 mJ/cm^2, respectively. The repetition rate was 0.67 Hz. The delay time was 0, 0.1, 0.5, and 1.4 s.

lieved that the broadening of absorption peaks comes from the inhomogeneous size distribution. The absorption spectrum of Fig. 9(a) is so broad that the peak is smeared. The shoulder indicated by an arrow corresponds to the blueshift of 26 meV, which is equal to the exciton quantum confinement energy in CuCl nanocrystals whose radius is 2.8 nm. This estimated value on the basis of Eq. (1) almost agrees with the mean radius, 2.7 nm, obtained by the small-angle x-ray-scattering measurement.

Figures 8(b) and 9(b) show the time dependence of DAS at 2 K in CuCl nanocrystals embedded in glass and in NaCl, respectively. These spectra were obtained by means of the same experimental procedures that were used for CdSe in GeO_2 glass. The excitation energy was 3.237 eV. The excitation density was 1.0 mJ/cm^2 and 1.5 mJ/cm^2 for CuCl in glass and in NaCl, respectively. Main spectral holes, antiholes, and satellite holes are clearly observed in DAS of CuCl in glass [Fig. 8(b)]. Antiholes are located at both sides of the main spectral holes and satellite holes are located at the low-energy shoulder of spectral holes. The satellite holes are found to originate from the first-order acoustic phonons confined in nanocrystals.[19] The DAS of CuCl in NaCl [Fig. 9(b)] also have structures, such as spectral holes, satellite holes, and antiholes. These spectral holes are broader than those of the CuCl in glass sample. The satellite holes observed at both sides of the main bleaching hole come from the first-order acoustic phonons confined in nanocrystals and the satellite holes observed at the lower-energy part probably come from the higher-order confined acoustic phonons.[19] The most important point shown in Figs. 8 and 9 is that the spectral holes and the other structures are observed at 1.4 s after the excitation. Moreover, we can observe the spectral holes for a few hours after the excitation. Therefore, we concluded that the long-lived spectral holes observed in two kinds of CuCl nanocrystals also come from the PSHB process.

Figures 10(a) and 11(a) show 77 K linear absorption spectra of CuCl nanocrystals in glass and NaCl, respectively. The time dependence of DAS at 77 K is also shown in Figs. 10(b) and 11(b). The samples were directly immersed in liquid nitrogen. The excitation energy and the excitation energy density were 3.263 eV and 1.5 mJ/cm^2 for CuCl nanocrystals embedded into glass, 3.254 eV and 1.5 mJ/cm^2 for CuCl nanocrystals embedded into NaCl, respectively. In CuCl nanocrystals, the linear absorption spectrum at 77 K shows blueshift compared with that at 2 K. The DAS of CuCl nanocrystals in glass [Fig. 10(b)] shows spectral holes and antiholes at both sides of holes. The spectral holes at 77 K are broader compared with those at 2 K and satellite holes are invisible. During 0.1 s after the excitation, the spectral hole slightly decreases. However, these structures, spectral holes, and antiholes, almost remain at 1.4 s after the excitation. On the contrary, the spectral hole of CuCl nanocrystals in NaCl [Fig. 11(b)] quickly decreases during 66 ms after excitation. The spectrum at 934 ms still has small structures which are similar to that at 66 ms. These results of Figs. 10 and 11 show that the PSHB phenomenon exists even at 77 K.

The upper part and the lower part of Fig. 12 show the temporal change in the spectral hole depths for CuCl nanocrystals in glass and in NaCl, respectively. The solid circles and the open circles indicate the depth of the spectral hole at 77 and 2 K, respectively. It can be seen from this figure that the relaxation of the spectral hole strongly

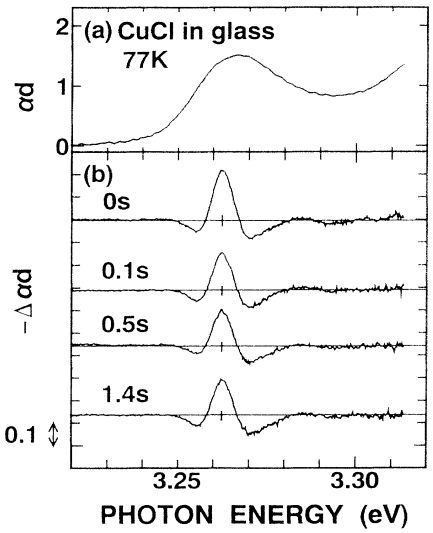

FIG. 10. (a) Linear absorption spectrum in CuCl nanocrystals embedded in glass at 77 K. (b) The time dependence of the differential absorption spectra in the same sample at 77 K. The excitation energy shown by vertical bars and the excitation energy density were 3.263 eV and 1.5 mJ/cm^2, respectively. The repetition rate was 0.67 Hz. The delay time was 0, 0.1, 0.5, and 1.4 s.

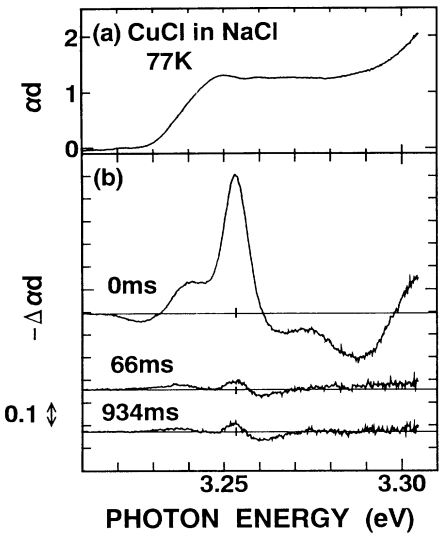

FIG. 11. (a) Linear absorption spectrum in CuCl nanocrystals embedded in NaCl at 77 K. (b) The time dependence of the differential absorption spectra in the same sample at 77 K. The excitation energy shown by vertical bars and the excitation energy density were 3.254 eV and 1.5 mJ/cm^2, respectively. The repetition rate was 1.0 Hz. The delay time was 0, 66, and 934 ms.

depends on temperature in case of CuCl nanocrystals in NaCl. Moreover, it is concluded that long-lived spectral holes due to the PSHB process were observed in CuCl nanocrystals embedded in two kinds of matrix at both 2 and 77 K.

C. Mechanism of the persistent spectral hole burning in semiconductor nanocrystals

So far, the temporal change of the spectral hole in semiconductor nanocrystals is explained by carrier relaxation processes from excited states. However, our results cannot be explained by the state filling of the excited states, because the spectral hole persists much longer than the lifetime of any of the excited states. In order to explain our results of the PSHB in semiconductor nanocrystals, more than one ground state is required. In glass containing organic molecules, the ground-state configurations are often referred to structural changes of molecules[23,26,27] and their environments.[29] Similarly, in semiconductor nanocrystals, many ground-state configurations can result from the production of persistent structural changes, such as changes in a nanocrystal surface or surrounding environments of nanocrystals, induced by the optical excitation. Next, we show an energy model to explain the PSHB in semiconductor nanocrystals qualitatively.

Figure 13 shows the schematic representation explaining the photophysical PSHB mechanism. Figures 13(a) and 13(b) represent the energy-level diagram. In Fig. 13(b), the ground states are represented as potential-energy wells for the explanation of the possible origin of persistency. The configuration of Fig. 13(b) is based on the generalization of the two-level-system model.[7] The excited state, the initial ground state, and the other ground states are represented by (E), (I), and (G), respectively. Site-selective excitation causes the transition from the initial ground state to the excited state and provides another ground-state configuration. The population at (G) is increased by the relaxation from (E). This causes the increase of the absorption at the both sides of spectral holes in the absorption spectrum. The increase of absorption is the so-called antihole. The relaxation time in the PSHB mechanism is mainly due to the relaxation from (G) to (I). A solid line and a dashed line in Fig. 13(c) show the absorption spectrum before and after the site-selective excitation, respectively. This PSHB model shown in Fig. 13 is called the "photophysical model."

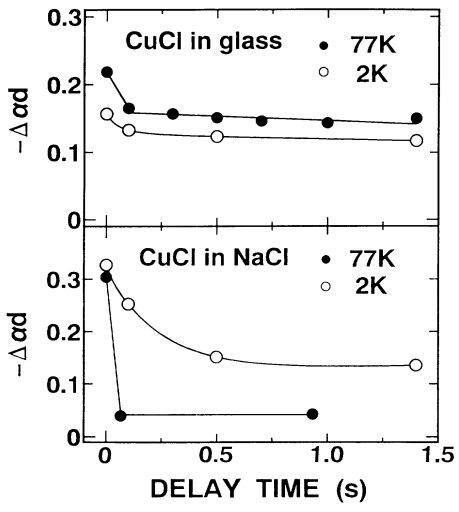

FIG. 12. The temporal change in the depth of spectral holes in CuCl nanocrystals embedded in glass and NaCl. The data were measured from the differential absorption spectra shown in Figs. 8–11. The solid circles (●) and the open circles (○) indicate the depth of spectral holes at 77 and 2 K, respectively.

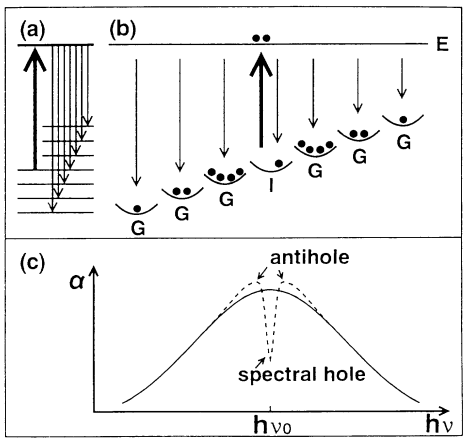

FIG. 13. The schematic representation of the persistent spectral hole-burning phenomenon based on the photophysical mechanism. (a), (b) The energy-level diagram. The excited state, the initial ground state, and the other ground states are represented by (E), (I), and (G), respectively. (c) A solid line and a dashed line show the absorption spectra before and after the site-selective excitation, respectively.

The overall absorption area integrated over the inhomogeneously broadened spectrum should remain approximately constant, because the site-selective excitation redistributes the population among the ground states. The conservation of absorption area is the essential point to ascribe the PSHB mechanism to the photophysical mechanism. In photochemical mechanism, on the contrary, the conservation is not satisfied and the absorption due to the photoproduct is observed.

Semiconductor nanocrystals studied in this work consist of 10^3-10^4 atoms. The number of atoms on the surface of nanocrystals is less than 20% of the total. Even if photochemical reaction takes place at the interface between nanocrystals and the surrounding matrix, the PSHB phenomenon is probably different from the photochemical PSHB phenomenon in molecular and ionic guests. We cannot imagine the photochemical change takes place in whole nanocrystals. The probable result is the reduction of the effective radius of nanocrystals which reduces the total area of the absorption spectrum. Therefore, it is rather difficult to distinguish the photochemical process from the photophysical one. The energies of the photoproducts are expected to be very close to the energies of burned nanocrystals. Photoproducts can give the antihole structures shown in Fig. 13(c). In this case, we can use the "photophysical model" shown in Fig. 13 even for the photochemical mechanism. Photoproducts are regarded as ground-state configurations.

According to the "photophysical model," we can explain the persistency of the antiholes in the DAS shown in previous subsections. In CdSe nanocrystals embedded into GeO_2 glass, therefore, the antiholes in Fig. 1 originate from the above-mentioned mechanism of the PSHB. It can be seen from the DAS of Figs. 1(a)–1(c) that the antiholes are not observed in the transparent region of CdSe nanocrystals in GeO_2 glass. This phenomenon is explained by the absence of the ground-state configuration at the transparent energy region, because ground-state configurations are considered to contribute also to the inhomogeneously broadened absorption spectra. This idea sharply contradicts with the generally accepted model of inhomogeneous broadening of semiconductor nanocrystals which takes account of the size distribution as the unique origin of the inhomogeneous broadening. The generally accepted model cannot be used for explanation of the PSHB phenomenon.

The conservation of the absorption area should be discussed in reference to the question whether the photophysical mechanism or the photochemical mechanism works. The conservation of the absorption area is not satisfied within the observed spectral range in Figs. 5(b) and 5(c), which was measured in CdSe nanocrystals. Therefore, the photochemical mechanism is working in CdSe nanocrystals. The photophysical mechanism is more suitable for the explanation of the DAS measured in CuCl nanocrystals embedded into glass. The structures of the DAS in Figs. 8 and 10 resemble those of Fig. 13(c). Figure 8 shows that the ratio of the antihole area to the hole area is 0.76 at 0 s, 0.78 at 0.1 s, 1.0 at 0.5 s, and 1.1 at 1.4 s. Similarly, Fig. 10 shows that the ratio is 0.77 at 0 s, 0.96 at 0.1 s, 1.1 at 0.5 s, and 1.1 at 1.4 s. In both cases, the conservation of the absorption area is almost satisfied at the later time stage. In the case of CuCl nanocrystals embedded in NaCl, the DAS have rich structures, spectral holes, antiholes, and satellite holes. Therefore, the structures of DAS strongly depend on the matrix. Although the antiholes were observed, the structures of spectra are a little different from those of Fig. 13(c). The absorption area is not conserved in the CuCl nanocrystals embedded in NaCl sample, either. The photophysical model well explains the antihole structure observed in CuCl nanocrystals, but some parts of the PSHB are due to the photochemical mechanism.

The satellite holes coming from the phonon sideband observed in CdSe and CuCl nanocrystals in glass or a crystal are explained in the framework of the PSHB phenomenon.[29] The Stokes satellite holes grow with the increase in the pump intensity. The essential point to account for this behavior of the Stokes phonon sideband is the saturation of the zero-phonon hole due to the finite number of certain-size nanocrystals and the burning of the larger-size nanocrystals with the help of phonon emission. The anti-Stokes phonon sideband arises, because the probe absorption associated with the emission of phonons is reduced by the presence of the zero-phonon hole.

At present, we cannot assign the definitive physical process responsible for the PSHB phenomenon presenting in the nanocrystals and matrix. However, we can mention two possible mechanisms. The first mechanism is the change of the stress coming from the matrix. The photons excite the spherical acoustic mode confined in nanocrystals which may induce the mechanical change of the interface between nanocrystals and matrix or the surrounding matrix itself. The second mechanism is the photoionization of nanocrystals caused by the trapping of electrons or holes at the interface or matrix. The identification requires further study.

D. Demonstration of optical data storage

Soon after the first observation of the PSHB, it was quickly recognized that spectral holes could be used for the high-density optical memory.[7,44] The presence or absence of a hole at a given energy within the inhomogeneous line could be used to encode a digital "1" or "0." When the homogeneous linewidth Γ_h is sufficiently narrow compared with the inhomogeneous broadening, many bits could be stored in a diffraction-limited laser spot. This type of memory, therefore, is a good candidate for ultrahigh-density memories that will be required in the near future. Here, optical multifrequency memory using the PSHB phenomenon is demonstrated in semiconductor nanocrystals. The CuCl nanocrystals in glass were selected as a sample for the demonstration because the width of the spectral hole of this sample was the narrowest in our samples.

The upper part and the lower part of Fig. 14 show the linear absorption spectrum and the DAS in CuCl nanocrystals embedded in glass at 2 K, respectively. The DAS was obtained by the excitation at three different photon energies, 3.236, 3.244, and 3.253 eV in turn. The excita-

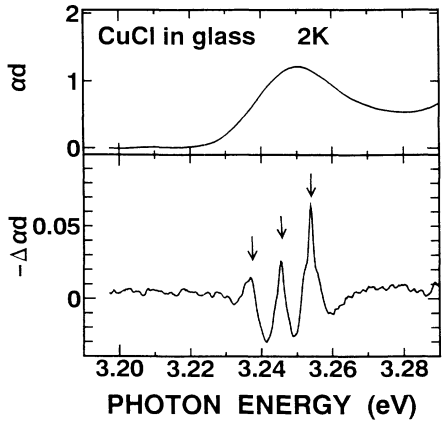

FIG. 14. (a) Linear absorption spectrum in CuCl nanocrystals embedded in glass at 2 K. (b) The differential absorption spectrum for the demonstration of the optical data storage. The excitation energy denoted by arrows was 3.236, 3.244, and 3.253 eV. The excitation energy density was 50 $\mu J/cm^2$.

tion energy density was 50 $\mu J/cm^2$. The same spot of the sample was excited by 2000 shots of the pump pulses at each excitation photon energy. After that, the DAS was simultaneously measured by probe pulses. Therefore, three spectral holes are observed at the different energy positions. Because the later excitation energy fills the hole burned by the previous excitation energy, the hole depth depends on the excitation history. Because the ratio of a spectral-hole width to the width of inhomogeneous broadening is not so small, it is rather difficult to make the spectral hole much more dense in the spectral range than this demonstration. Although the present result is not enough for practical application, we cannot deny the possible capabilities of semiconductor nanocrystals for the optical memory in the future.

V. CONCLUSIONS

We studied the spectral hole burning in semiconductor nanocrystals by means of the nanosecond pump-and-probe technique. According to time-dependent measurements of the DAS, spectral holes, antiholes, and satellite holes were observed even at 1.4 s after the excitation at 2 K for three samples, CdSe nanocrystals in GeO_2 glass, CuCl nanocrystals in silica-rich glass, and CuCl nanocrystals in NaCl. Moreover, these structures remained after a few hours at 2 K. Even at 77 K, long-lived spectral holes were observed for CuCl nanocrystals in glass and in NaCl. The formation process of long-lived spectral holes can be explained by considering the PSHB process. In $CdS_{0.59}Se_{0.41}$ nanocrystals in glass, the PSHB phenomenon was observed, too. Our results are the first observation of the PSHB in semiconductor nanocrystals. The "photophysical model" explains fairly well the antihole structures in the PSHB spectra.

Semiconductor nanocrystals consisting of 10^3–10^4 atoms behave like molecules in the matrix to give the PSHB phenomenon, which has been missed by many previous authors. This finding gives a different aspect to the physics of mesoscopic semiconductor structures. Many kinds of semiconductor nanocrystals can be new media for persistent hole-burning spectroscopy. The PSHB phenomenon seriously contributes to the nonlinear optical measurement of semiconductor nanocrystals. Moreover, many previous data about nonlinear optical properties of semiconductor nanocrystals should be reexamined.

ACKNOWLEDGMENTS

The authors wish to thank Professor T. Arai of University of Tsukuba for kindly providing the samples of CdSe in GeO_2 glass. Small-angle x-ray-scattering experiments were done by the approval of the Photon Factory (PF) Advisory Committee (Proposals 90-222 and 92-117). The authors wish to thank Professor Y. Amemiya in PF for his kind guidance to the small-angle x-ray-scattering experiments. The experiments at PF were performed by collaboration with S. Katayanagi, T. Kawazoe, S. Okamoto, and K. Kawabata. The authors deeply thank them. This work is supported by the New Energy and Industrial Technology Development Organization (NEDO) of Japan.

*Present address: Fiber Optics Division, Central Research Laboratory, Hitachi Ltd., Kokubunji, Tokyo 185, Japan.
†Present address: Stepanov Institute of Physics, F. Skaryna Ave., 70 Minsk 220072, Belarus.
‡Author to whom correspondence should be addressed.

[1]A. I. Ekimov, Al. L. Efros, and A. A. Onushchenko, Solid State Commun. **56**, 921 (1985).
[2]L. Brus, IEEE J. Quantum Electron. **QE-22**, 1909 (1986).
[3]A. D. Yoffe, Adv. Phys. **42**, 173 (1993), and references therein.
[4]R. K. Jain and R. C. Lind, J. Opt. Soc. Am. **73**, 647 (1983).
[5]S. Schmitt-Rink, D. A. B. Miller, and D. S. Chemla, Phys. Rev. B **35**, 8113 (1987).
[6]E. Hanamura, Phys. Rev. B **37**, 1273 (1988).
[7]*Persistent Spectral Hole-Burning: Science and Applications*, edited by W. E. Moerner, Topics in Current Physics Vol. 44 (Springer-Verlag, Berlin, 1988).
[8]Y. R. Shen, *The Principle of Nonlinear Optics* (Wiley, New York, 1984).
[9]P. Roussignol, D. Ricard, C. Flytzanis, and N. Neuroth, Phys. Rev. Lett. **62**, 312 (1989).
[10]A. P. Alivisatos, A. L. Harris, N. J. Levinos, M. L. Steigerwald, and L. E. Brus, J. Chem. Phys. **89**, 4001 (1988).
[11]M. G. Bawendi, W. L. Wilson, L. Rothberg, P. J. Carroll, T. M. Jedju, M. L. Steigerwald, and L. E. Brus, Phys. Rev. Lett. **65**, 1623 (1990).
[12]N. Peyghambarian, B. Fluegel, D. Hulin, A. Migus, M. Joffre, A. Antonetti, S. W. Koch, and M. Lindberg, IEEE J. Quantum Electron. **QE-25**, 2516 (1989).
[13]S. H. Park, R. A. Morgan, Y. Z. Hu, M. Lindberg, S. W. Koch, and N. Peyghambarian, J. Opt. Soc. Am. B **7**, 2097 (1990).
[14]T. Wamura, Y. Masumoto, and T. Kawamura, Appl. Phys.

Lett. **59**, 1758 (1991).
[15]U. Woggon, S. Gaponenko, W. Langbein, A. Uhrig, and C. Klingshirn, Phys. Rev. B **47**, 3684 (1993).
[16]K. I. Kang, A. D. Kepner, S. V. Gaponenko, S. W. Koch, Y. Z. Hu, and N. Peyghambarian, Phys. Rev. B **48**, 15 449 (1993).
[17]S. Nomura and T. Kobayashi, Phys. Rev. B **45**, 1305 (1992).
[18]T. Itoh and M. Furumiya, J. Lumin. **48&49**, 704 (1991).
[19]S. Okamoto and Y. Masumoto, J. Lumin. (to be published).
[20]P. Gilliot, J. C. Merle, R. Levy, M. Robino, and B. Hönerlage, Phys. Status Solidi B **153**, 403 (1989).
[21]Y. Masumoto, T. Wamura, and T. Kawamura, Surf. Sci. **267**, 315 (1992).
[22]Y. Masumoto, L.G. Zimin, K. Naoe, S. Okamoto, and T. Arai, Mater. Sci. Eng. B (to be published).
[23]A. A. Gorokhovskii, R. K. Kaarli, and L. A. Rebane, Pis'ma Zh. Eksp. Teor. Fiz. **20**, 474 (1974) [JETP Lett. **20**, 216 (1974)].
[24]R. M. Macfarlane and R. M. Shelby, Phys. Rev. Lett. **42**, 788 (1979).
[25]R. M. Macfarlane and J.-C. Vial, Phys. Rev. B **34**, 1 (1986).
[26]T. Tani, H. Namikawa, K. Arai, and A. Makishima, J. Appl. Phys. **58**, 3559 (1985).
[27]W. Breinl, J. Friedrich, and D. Haarer, Phys. Rev. B **34**, 7271 (1986).
[28]H. de Vries and D. A. Wiersma, Phys. Rev. Lett. **36**, 91 (1976).
[29]G. J. Small, in *Spectroscopy and Excitation Dynamics of Condensed Molecular Systems*, edited by V.M. Agranovich and R. M. Hochstrasser (North-Holland, Amsterdam, 1983), p. 515.
[30]W. E. Moerner, A. R. Chraplyvy, A. J. Sievers, and R. H. Silsbee, Phys. Rev. **28**, 7244 (1983).
[31]R. W. Olson, H. W. H. Lee, F. G. Patterson, M. D. Fayer, R. M. Shelby, D. P. Burum, and R. M. Macfarlane, J. Chem. Phys. **77**, 2283 (1982).
[32]W. E. Moerner, A. J. Sievers, R. H. Silsbee, A. R. Chraplyvy, and D. K. Lambert, Phys. Rev. Lett. **49**, 398 (1982).
[33]A. Tanaka, S. Onari, and T. Arai, Phys. Rev. B **45**, 6587 (1992).
[34]L. G. Zimin, S. V. Gaponenko, V. Yu. Lebed, I. E. Malinovskii, I. N. Germanenko, E. E. Podorova, and V. A. Tsekhomskii, Phys. Status Solidi B **159**, 267 (1990).
[35]D. Bersani and P. P. Lottici, Phys. Status Solidi B **174**, 575 (1992).
[36]Y. Masumoto, T. Wamura, and T. Kawamura, Appl. Phys. Lett. **58**, 2270 (1991).
[37]Y. Masumoto, T. Kawamura, and K. Era, Appl. Phys. Lett. **62**, 225 (1993).
[38]Y. Masumoto, T. Katayanagi, and T. Mishina, Phys. Rev. B **49**, 10 782 (1994).
[39]V. V. Golubkov, A. I. Ekimov, A. A. Onushchenko, and V. A. Tsekhomskii, Sov. J. Glass Phys. Chem. **8**, 265 (1982).
[40]Y. Z. Hu, M. Lindberg, and S. W. Koch, Phys. Rev. B **42**, 1713 (1990).
[41]Long-lived (~ 2 μs) induced absorption was reported for CdTe nanocrystals embedded in glass [V. Esch *et al.*, Phys. Rev. B **42**, 7450 (1990)]. Authors claimed that the induced absorption structure comes from the transition to the two-electron-hole state. They considered the long life of the induced absorption structure is not inconsistent with the two-electron-hole pair model.
[42]*Numerical Data and Functional Relationships in Science and Technology*, Physics of II-VI and I-VII Compounds, Semimagnetic Semiconductors, edited by O. Madelung, Landolt-Börnstein, New Series, Group III, Vol. 17, Pt. b (Springer-Verlag, Berlin, 1982).
[43]M. G. Bawendi, P. J. Carroll, W. L. Wilson, and L. E. Brus, J. Chem. Phys. **96**, 946 (1992).
[44]A. Szabo, U.S. Patent No. 3,896,420 (1975).